Comparative assessment of the performances of GPS-TEC assisted NTCM, NeQuick2 and Neural Network models to describe the East-African equatorial Ionosphere

B. Getahun[1], M.Nigussie [1], A.Tebabal [1]

[1]Washera Geospace and Radar Science Laboratory, Bahir Dar University, Bahir Dar, Ethiopia

Abstract

Different ionospheric climatological models such as NeQuick2 and NTCM have been developed to mitigate the ionosphere impact on the trans-ionosphere propagating radio wave. Moreover, the Neural Network (NN) is used to model and characterize the ionosphere. However, no one has compared the performances of NeQuick2, NTCM, and NN after adapting to GPS TEC. This study evaluates their performances in the East-African region in 2013 and 2015. It has been done by computing their drivers (effective ionization level, Az for NeQuick2 and ionization driving index, Id for NTCM) through least-square fitting to TEC observation sense. NN-algorithm has also been trained and tested with observed TEC used for NeQuick2 and NTCM adaptation. The annual performance test has shown that the correlation coefficient (R) values between observed and NTCM modeled TEC, after an adaption, are better than the corresponding values obtained from NeQuick2 and NN. It also shows that the standard deviations (STD) and root-mean-square errors (RMSE) obtained for NTCM are smaller than the STD and RMSE computed for NeQuick2 and NN. On the other hand, the daily performance test of now-casting and predicting showed that the NN performs the best, followed by NTCM. However, the 1-hour prediction test showed that NTCM performs the best among the models considered in this study.

Key Words: NTCM, NeQuick2, NN, TEC, Data ingestion, and Model Performance.

Key points: When NTCM is assisted by extended data, it performs better than assisted NeQuick2 and NN models.

1. Introduction

The ionosphere is part of the upper atmosphere of Earth where EUV, X-ray radiations, and energetic particles from the sun ionize the atoms and molecules. It is a region where free electrons occur in a high enough density to influence the propagation of radio waves with measurable effects. It is one of the highly variable regions of the Earth-upper atmosphere. Nowadays, society has become reliant on systems that work with communication of the satellites whose performance is dependent on the state of the ionosphere. The ionosphere causes a significant error in single-frequency GPS navigation (Tiwari et al., 2013, Davies, 1990). The temporal and spatial variation of electron density (total electron content, TEC) of the ionosphere affects the GPS signal propagation by introducing delay (slowing down and bending propagation) and scintillation (Kouris et al., 2004; Tulunay et al., 2004, 2006; Jakowski et al., 2012; Opperman et al.,

2007). Understanding the ionosphere dynamics and developing a model for now-casting and forecasting its TEC might mitigate the ionosphere effect. In this regard, the interest in specifying the ionosphere TEC is not only for climatic-like situations but also for weather-like behavior.

Global empirical models such as IRI (Bilitza et al., 2018), NeQuick2 (Nava et al., 2008), and NTCM (Jakowski et al., 2011) are good in capturing the median behavior of the ionosphere. These models have been designed for scientific study and radio communication applications. For example, NeQUick2 is adopted for TEC prediction to improve communication quality for International Telecommunication Union Radiocommunication Sector (ITU-R). It is also approved to be used for single frequency ionospheric error correction in the framework of GALILEO (Nigussie et al., 2012 and references therein). These models have shown different performance in their standard application in describing the observed TEC; for example, Nigussie et al. (2013) have compared the performance of NeQuick2 and IRI-2007 models in describing the East-African ionospheric TEC and found, for both models, the modeled and experimental VTEC has shown significant discrepancy. The performance of NTCM in its standard applications has shown also a significant discrepancy to the experimental VTEC (Getahun and Nigussie, 2021). The weak performances of these models in their standard applications indicate limitations in reproducing and forecasting the local and instantaneous conditions, especially in regions of unique irregularities are common (Scherliess et al., 2004; Sojka et al., 2007).

We have adapted Empirical models to GPS TEC in different longitudinal sectors to upgrade their weak performances. Studies showed that TEC ingestion into the NeQuick2 model improves its performance in reproducing spatial and temporal variations of the ionosphere TEC and electron density (Nava et al., 2006, 2011; Brunini et al., 2011; Nigussie et al., 2012; Ercha et al., 2018). Similarly, Getahun and Nigussie (2021) showed that adapting the NTCM model to quiet days TEC in the East-Africa ionosphere improved its performance substantially. Also, to enhance ionosphere characterization for scientific research, and mitigate its effect on positioning and communication, the Neural Network (NN) model has been suggested by various studies (Habarulema et al., 2007, 2009; Tebabal et al., 2018, 2019).

For instance, Habarulema et al. (2007, 2009) and Tebabal et al. (2018) developed a regional model by training the NN algorithm to GPS TEC obtained in South and East African sectors and compared the output of their model with the IRI-2001 and NeQuick2 standard applications, respectively and found that the regional NN model performed better than the IRI-2001 and NeQuick2. Searching model that can compute TEC faster with better performance is still the demand for the scientific community in the discipline. Therefore, it is substenial to assess the performances of NN, NeQuick2, and NTCM models after adapting them to ionospheric TEC observations. To our best knowledge, no body has yet compared NN model, NeQuick2, and NTCM after and even before adapting them to ionospheric measurements.

The main objective of this study is to compare the performance of data-assisted NTCM with that of adapted NeQuick2 models and NN in estimating GPS - VTEC in the East African sector. In addition, this work provides background for the quest of developing a forecasting VTEC model in the East African equatorial ionosphere. We used hourly VTEC from 19 GPS stations in East Africa and then analyzed the performance of adapted NeQuick2, adapted NTCM, and trained NN in reconstructing the VTEC.

2) Ionospheric Models used

2.1 NTCM Model

NTCM model developed at Neustrelitz, Germany institution of Communication and Navigation, DLR provides a simple and easily accessible representation of VTEC varying with time and location under the varying condition of solar activity. It combines functions defined on the geographic location (latitude and longitude), time (hour of a day and day of a year), and solar activity represented by F10.7, and it estimates VTEC (Jakowski et al., 2011). It describes diurnal variations, seasonal variations, equatorial latitude anomaly, and solar flux dependency using harmonic functions with 12 linear coefficients. Detail mathematical formulations are available in Jakowski et al. (2011).

2.2 NeQuick2 Model

NeQuick2 is a three-dimensional time-dependent empirical model derived from the profile proposed by Di Giovanni and Radicella (1990). The development of the NeQuick2 model was at the Aeronomy and Radiopropagation Laboratory of the Abdus Salam International Centre for Theoretical Physics (ICTP), Trieste, Italy, and the Institute for Geophysics, Astrophysics, and Meteorology of the University of Graz, Austria (Brunini et al., 2011; Nava et al., 2008). It is complex compared to the NTCM model. Six semi-Epstein functions, which are defined by maximum electron density (Nm) and height of maximum electron density (hm) of E, F1, and F2 layers of the ionosphere as anchor points (Nava et al., 2008), frame the model. Five of them with thickness parameters of the model describe the lower and upper parts of E & F1 and the lower part of the F2 region. The sixth function with the height-dependent thickness parameter formulates the topside ionosphere. Positions of receiver and satellite, time, and solar flux (sunspot number) are inputs of the NeQuick2 model, while the electron density profile is the output.TEC is also estimated numerical integration of the electron density along a path joining the receiver and satellite.

2.3 Neural Network (NN)

The neuron cells of the biological nervous system take inputs, process them, and produce a response. Similarly, a neural network (NN) is an information processing mathematical structure designed for non-linear data-driven estimation (Haykin, 1999; Habarulema et al., 2007; Tebabal et al.,2018). NN consists of parallel computing basic units (nodes). These nodes are organized as input layer, the hidden layers, and the output layer (see Figure 1).The data fed to

the nodes of the input layer pass to the nodes of hidden layer/s and then to the output layer by computing output at each node using transformation and activation functions. The transformation function is a simple weighted linear combination of the values of nodes of the previous layer. The activation function determines the output of a node using the transformation function results as input. Consecutive operations of these functions continue from the first hidden layer to the output layer to compute the model output. Weights, that connected nodes of adjacent layers, and biases of a node are updated through backprop-agation of error (the difference between model output and target data) during training. The input layer has nodes equal to the number of the independent variables of the problem. The output layer nodes are the same as the dependent variables of the problem. The network might have one or more hidden layers with some nodes determined from the model performance for a particular data. For example, this study includes the sine of hours of the day, cosine of hours of the day, the sine of days of the year, cosine of days of the year, geographic lati-tude, longitude, and solar index represented by F10.7 for independent variables. The dependent variable is VTEC. Thus, the nodes of the input layer are seven, and in the output layer, is only one. In this study, we used NN consisting of two hidden layers of 8 and 6 nodes for the training. We determine the number of hidden layers and nodes by trials for the best performance.
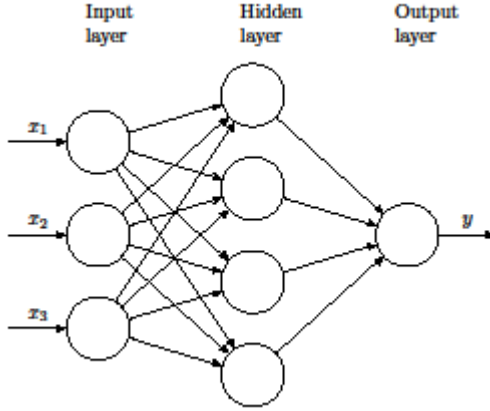

Figure 1: Schematic of neurons in a sample of single hidden layer feed forward neural network.

The feeding forward and backpropagation process minimizes the error (the dif-ference between the observed and modeled values) to a tolerable level. The training is to reduce the mean square error defined in equation 1.

$$E_D = \frac{1}{N}\sum_{i=1}^{N}\left(\text{VTEC}_{\text{obs}}^i - \text{VTEC}_{\text{NN}}^i\right)^2 , (1)$$

where, N is the number of observations; $\text{VTEC}_{\text{obs}}^i$ and $\text{VTEC}_{\text{NN}}^i$ are observation and model VTECs, respectively.

This study adopted the feed-forward neural network with Bayesian backpropagation (MacKay, 1992). The method offers a significant advantage over the standard backpropagation algorithm by reducing the lengthy cross-validation (Burden and Winker, 2009). In the Bayesian regularization algorithm, the objective function includes two terms as expressed by equation 2.

$$J(W) = \alpha E_w + \beta E_D \ . \ (2)$$

Here, α and β are parameters used for regularization that will be determined from Bayesian computation (MacKay, 1992). $E_w = \frac{1}{2} \sum_i^N w_i^2$ is weight decay.

The Bayesian approach considers the weights as random variables. So the density function is defined by Baye's rule as:

$$P(W/D, \alpha, \beta, M) = \frac{p(D/W,\alpha,\beta,M)p(W/\alpha,\beta,M)}{p(D/\alpha,\beta,M)} \ , \ (\ 3)$$

where, W is a vector of weight; D is data used and M is the network. Moreover, $P(D/W, \alpha, \beta, M)$ is likelihood function of the data given such as W and M. $P(D/\alpha, \beta, M)$ is the normalization function and $P(W/\alpha, \beta, M)$ is the priority density function that represents our prior believes.

By assuming Gaussian distribution errors in the training, the probability density function becomes

$$P(W/D, \alpha, \beta, M) = \frac{1}{Z_J(\alpha,\beta)} e^{-J(W)} \ . \ (\ 4)$$

In this framework, the optimal weight is equivalent to minimizing the objective function.

For details of Bayesian regularization, interested readers can see different studies (Foresee and Hagan, 1997; MacKay, 1992; Duhoux et al., 2001; Khan and Coulibaly, 2006; Burden and Winkler, 2009; Soudry and Meir, 2013; Hernández-Lobato and Adams, 2015; Ghosh and Doshi-Velez,2017; Tebabal et al.2019).

3 Method and data

3.1 Method

3.1.1 Data Ingestion

Both NTCM and NeQuick2 model VTECs are a monotonic function of the 10.7 cm radio flux (F10.7). Local and instantaneous values of F10.7 defined for NeQuick2 effective ionization (symbol Az) and NTCM ionization driving index (symbol Az) are F10.7 values that minimize the difference between an experimental and the corresponding modeled VTEC. Many works of literature (Nigussie et al., 2012, Ercha et al., 2018, Nava et al., 2006, Getahun and Nigussie, 2021) reviewed that Id or Az is estimated by minimizing the root mean square error (RMSE) defined in equation 5.

$$\text{RMSE (Id or Az)} = \sqrt{\frac{\sum_i^N (VTECm_i(Id \ or \ Az) - \text{VTECo}_i)^2}{N}}, \ (5)$$

where, VTECm$_i$ (Id or Az) is the model VTEC computed as function of Id for NTCM or Az for NeQuick2, VTECo$_i$ is measured VTEC, and N is the number of satellites visible in an epoch of time. One of the values of F10.7 in a range used to run NTCM or NeQuick2, which minimizes equation (5) for each hour of measurements, is taken to be the Id or Az of the hour of the day. Then the model VTEC after data ingestion is calculated using the Id or Az.

3.1.2 Neural Network Training

The training of the NN is a process of calculating errors (the difference between the NN modeled and observed VTECs) by backpropagating them to calculate the gradient with the weights, then adjusting and updating them in an iterative approach. The data (inputs and the targets) are used for training and testing the model. With the training data, the network runs to determine the error. This error then propagates from the output layer through hidden layers to the input layer for updating weights and biases. Fausett (1994) discussed the technical details of the backpropagation algorithm well. We use different statistical parameters for the analysis of the error: the root means squared error (RMSE), the mean absolute error (MAE), standard deviation (STD), and correlation coefficient (R) (Pooleand McKinnell, 2000; Habarulema et al., 2009; Lamming and Cander,1999; Razin et al., 2016).

We used the inputs and targets data for training (100%) and simulating (100%). The input data day of the year (DOY) and hour (HR) are converted into sine and cosine to make sure that the data is cyclic continuous (Habarulema et al., 2009; Tebabal et al.2019).

DNS $= \sin\left(\frac{2\,\mathrm{DOY}}{365.25}\right)$ (6) DNC $= \cos\left(\frac{2\,\mathrm{DOY}}{365.25}\right)$ (7)

HRS $= \sin\left(\frac{2\,\mathrm{HR}}{24}\right)$ (8) HRC $= \cos\left(\frac{2\,\mathrm{HR}}{24}\right)$ (9)

where DOY is the number of day in the year and HR is the hour in the day.

We considered days of the year (DOYs) in 2013 and 2015 with an Ap index of less than 15. So the work is limited to non-magnetic storm conditions.

3.1.3 Vertical TEC mapping Techniques

We used NTCM, NeQuick2, NN and direct VTEC interpolation to develop maps of VTEC for the East African region. We included Nineteen GPS stations' data (see Table 1 for their coordinates) for data ingestion (NTCM &NeQuick2 models), for training the NN and interpolation. The Id and Az values estimated at each IPP for every hour using equation (5) in the IPP plane are represented by a function that varies in latitude and longitude. The polynomial used is formulated from linear variation in longitude ( ) and quadratic variation in latitude ( ), and it is expressed by

Id $(\vartheta, \lambda) = a_0 + a_1\vartheta + a_2\lambda + a_3\ + a_4\vartheta^2$ (10)

where, the a$_i$'s are coefficients of the polynomial and they are estimated from the Id values applying the least-square fitting technique. Once these coefficients

6

are estimated, equation (10) has been employed to estimate the map of Id to drive NTCM to compute the map of VTEC after data ingestion. And then, the VTEC has been estimated at any latitude and longitude to produce the VTEC map. The corresponding VTEC for NeQuick2 models has been mapped by running it in the same region using Az values derived using equation 10. Similarly we ran NN-model trained by data used in equation (10) for mapping VTEC using NN. The models performances in estimating the VTEC map has been compared with observed VTEC map.

3.2 Data

The GPS receivers in East Africa create a platform to check the performance of global models, develop local models, and study the ionosphere in the East African sector. In this particular study, we used 19 receivers in the region. Table1 shows their geographic locations. We calibrated the GPS RINEX data using the technique discussed in Ciraolo et al. (2007). We computed the VTEC from the STEC mapping function described in *Mannucci et* al. (1998).

Table 1: Geographic and geomagnetic location of the GPS stations used for the study.

Stations	Code	Geographic		Geomagnetic		Dip –latitude
		Latitude (°N)	Longitude (°E)	Latitude (°N)	Longitude (°E)	
Bahir Dar	BDMT	11.60	37.36	8.07	111.48	3.63
Ambo	ABOO	8.99	37.81	5.44	111.50	0.78
Assosa	ASOS	10.05	34.55	7.00	108.48	1.50
Addis Ababa	ADIS	9.05	38.77	5.39	112.44	0.98
Arba Minch	ARMI	6.06	37.56	2.63	110.78	-2.53
Asab	ASAB	13.06	42.65	8.75	116.86	5.93
Asum	ASUM	-0.62	34.62	-3.49	106.82	-10.34
Debark	DEBK	13.15	37.89	9.58	112.24	5.44
Ginir	GINR	7.15	40.71	3.21	114.05	-0.88
Malindi	MAL2	-3.00	40.19	-6.74	111.96	-12.16
Mbarara	MBRA	-0.60	30.74	-2.83	102.99	-10.89
Eldoret	MOIU	0.29	35.29	-2.70	107.63	-9.24
Nazret	NAZR	8.57	39.29	5.01	112.9	-0.51
Negele	NEGE	5.33	39.59	1.59	12.66	-3.06
Nirobi	RCMN	-1.22	36.89	-4.45	108.97	-10.67
Robe	ROBE	7.11	40.03	3.7	113.37	-1.02
Seraba	SERB	12.51	37.02	9.08	111.28	4.61
Shimsheha	SHIS	11.99	38.99	8.26	113.12	4.29
Sheb	SHEB	15.85	39.05	12.06	113.81	8.60

For the multipath effect screening, we avoided data of elevation angle below 20°. The VTEC data are taken for relatively quiet days of the years 2013 and 2015. For both data ingestion and NN training, we used VTEC at each hour of the day.

However, for the training NN, we prepared the data as inputs and targets. The input consists of the factors that determine the variation of VTEC. The cosines and sines formulated by equations (6-9) refer to seasonal and diurnal variations of VTEC. In addition, the input included the latitude and longitude of IPP, and the daily F10.7, which represents the solar activity. Since we limited our study to relatively quiet days, we did not consider the geomagnetic index. The target is the VTEC at each hour. For annual performance, we used 2015 data at some sample stations (table1) for training and simulating. But for mapping, we used DOY 110 in 2013 data at stations mentioned in table 1. For diurnal variation, we chose only four days of the year 2015. For predication , the DOY 90 VTEC data is used.

4 Results and Discussion

4.1 Annual Performance of NTCM, NeQuick2 and NN models

We computed the NeQiuck2 and the NTCM VTEC using Ids and Azs and simulated NN after trained for the data used. The left panels of Figure 2 show the scattered plots of modeled VTEC versus observed VTEC for the Addis Ababa station in the year 2015. Plots in the panles are for NN, NeQuick2, and NTCM from top to bottom in order. The correlation coefficients determined for NTCM, NeQuick2, and NN models are 0.980, 0.953, and 0.956 in their order. The right panels present the corresponding histograms of error distributions with the standard deviation and root mean squared error (RMSE). As shown in the figure, the RMSE of NTCM (2.948 TECU) is much smaller than that of both the NeQuick2 (4.494 TECU) and NN models (4.372 TECU), which implies that NTCM performs better than the other models.

The NeQuick2 model shows relatively poor performance. The histograms of residuals approximately present symmetrical distribution on both sides of zero that demonstrates the characteristics of a normal distribution. In general, the scatter plots and the histograms depict that the models VTEC agrees with GPS_VTEC. However, their degrees of agreement are different. The NTCM model agrees the most. The NN model agrees better than that of the NeQuick2 model.
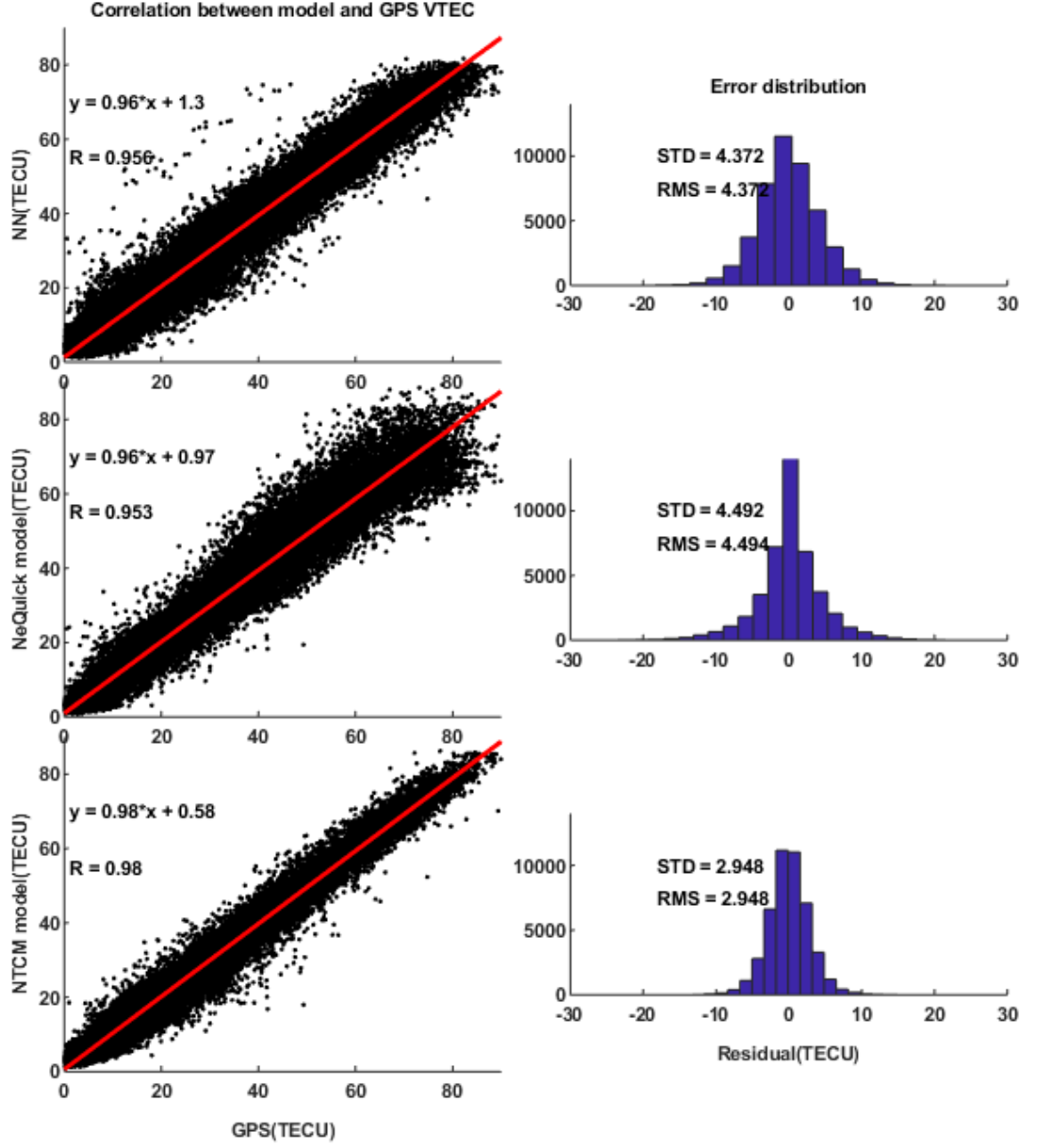
Figure 2: Scatter plot of modeled VTEC values versus observed GPS-VTEC (marked black dot) with the linear fit (red line) (left panels) and histogram of difference between model -VTEC and GPS-VTEC (right panels) for Addis Ababa station in 2015.

Figure 3 is the same as Figure 2 but for Arbaminch station. The results are similar to the Addis Ababa station, except for the numerical difference in the values of R, STD, and RMSE. Nevertheless, the NeQuick2 model performed a little bit better than the NN model in this station. R (STD & RMSE) for NTCM, NeQuick2 and NN models are 0.977 (2.107 & 2.107), 0.962 (3.561 & 3.564) and 0.954 (3.776 & 3.776), respectively.
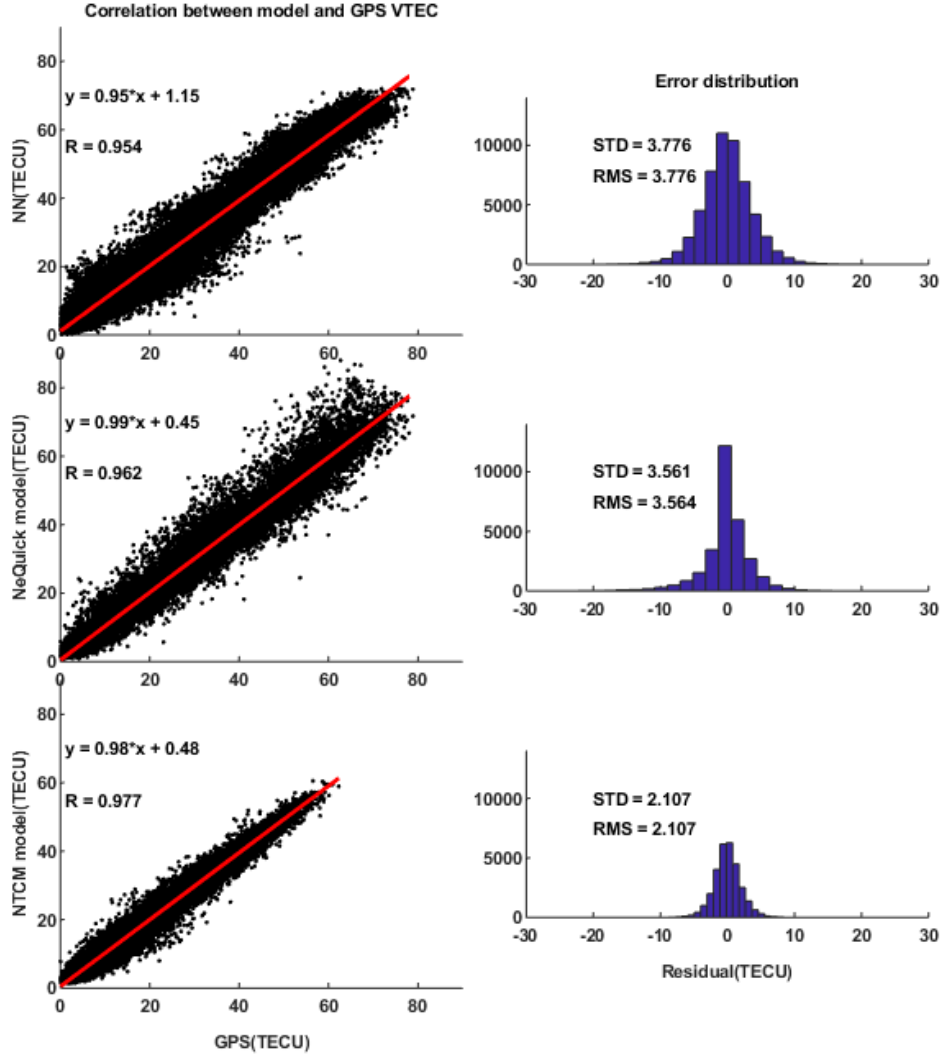

Fgure 3: Scatter plot of modeled VTEC values versus observed GPS-VTEC (marked black dot) with the linear fit (red line) (left panels) and histogram of difference between model -VTEC and GPS-VTEC (right panels) for Arbaminch

10

station in 2015.

Table 2: Statistical analysis summary over different stations in 2015:estimated R-values, STDs and RMSEs between GPS-VTEC and NTCM, NeQuick2 and NN –VTEC.

| Stations	Models	R-values	STDs	RMSEs
ABOO	NTCM	0.979	2.654	2.654
	NeQuick	0.942	3.742	3.764
	NN	0.949	4.063	3.958
MIOU	NTCM	0.937	4.206	4.206
	NeQuick	0.930	4.432	4.432
	NN	0.924	4.854	4.667
DEBK	NTCM	0.965	3.579	3.579
	NeQuick	0.938	4.789	4.790
	NN	0.944	4.485	4.449
ASOSA	NTCM	0.979	2.682	2.682
	NeQuick	0.955	3.981	3.997
	NN	0.954	4.067	3.972
SHIS	NTCM	0.972	3.354	3.354
	NeQuick	0.952	4.467	4.470
	NN	0.959	4.066	3.981
ASAB	NTCM	0.964	3.607	3.607
	NeQuick	0.901	6.209	6.246
	NN	0.942	4.558	4.423
GINR	NTCM	0.984	2.250	2.250
	NeQuick	0.967	3.298	3.303
	NN	0.958	3.679	3.602
NEGE	NTCM	0.981	2.459	2.459
	NeQuick	0.962	3.498	3.505
	NN	0.955	3.810	3.723
RCMN	NTCM	0.935	4.135	4.135
	NeQuick	0.936	4.126	4.132
	NN	0.917	4.905	4.696

For further verification of the performance of the models, we used nine more stations. Table2 summarizes the statistics of each station and each model. The correlation coefficients (shown in column 3 of Table 2) show that the models captured most of the experimental values. It ranges from 0.901-to 0.984.

However, the correlation coefficients for NTCM are better than the other two models. In addition to R, we used STD and RMSE to measure the performance of the models. In general, the performance of the models measured by STD and RMSE of the errors ranges to reasonable values. RMSEs range from 2.25-to 6.246. STDs are in the range from 2.25-6.209 TECU. These imply that the

models work well relative to the GPS observed VTEC. However, these values are much smaller for NTCM than for the other two models (NeQick2 and NN). The minimum (the maximum) STD for NTCM, NeQuick2, and NN are 2.25 (4.206) TECU, 3.988 (6.209) TECU, and 3.602 (4.696) TECU in their order. These results are comparable with the previous studies (Nigussie et al., 2012; Getahun and Nigussie, 2021; Tebabal et al.,2018) for these models, except for differences resulting from the data used.

4.2 VTEC Maps using Interpolation, NTCM, NeQuick2 and NN Models

Figures 4-6 display sample scatter plots (first column) of GPS observed VTEC and corresponding VTEC maps simulated by the models: Polynomial interpolation (second column), NTCM after adaptation (third column), NN (fourth column), and NeQuick2 after adaptation (fifth column) for DOY 110 in the year 2013 at 2hrs gap from 2-18 UTCs. In general, the models reproduced VTEC maps that capture the behavior of the scatter plots (experimental VTEC). However, they showed a difference in their performances. Since the scatter plot (experimental VTEC) for 2 UTC does not show much variation, the models' performances are unequivocal for these time. A littel variation for 4, 6, 8 & 18 UTCs experimental TEC have been reflected in the models (interpolation, NTCM, NN, and NeQuick2) maps with little difference among the performance of the models. However, for 10-16 UTCs, their performance differences are significant for the big experimental VTEC variation with geographic location. If we closely look at the plots, the polynomial interpolation and NTCM model results are much better in fitting to the scatter plots than the results of the NN and the NeQuick2 models. All approaches captured the EIA observed at 10, 12, 14, and 16 UTCs. However, there is some difference in clarity of EIA among models. The interpolation and NTCM model show clearer EIA observed in the experiment for these time intervals but the NN and NeQuick2 models have a little bit exaggerated the crests of EIA in the North and South hemisphere, which are depicted in the scatter maps (experimental). At 18 UTC the interpolation and NTCM magnified the observed EIA in the scattered
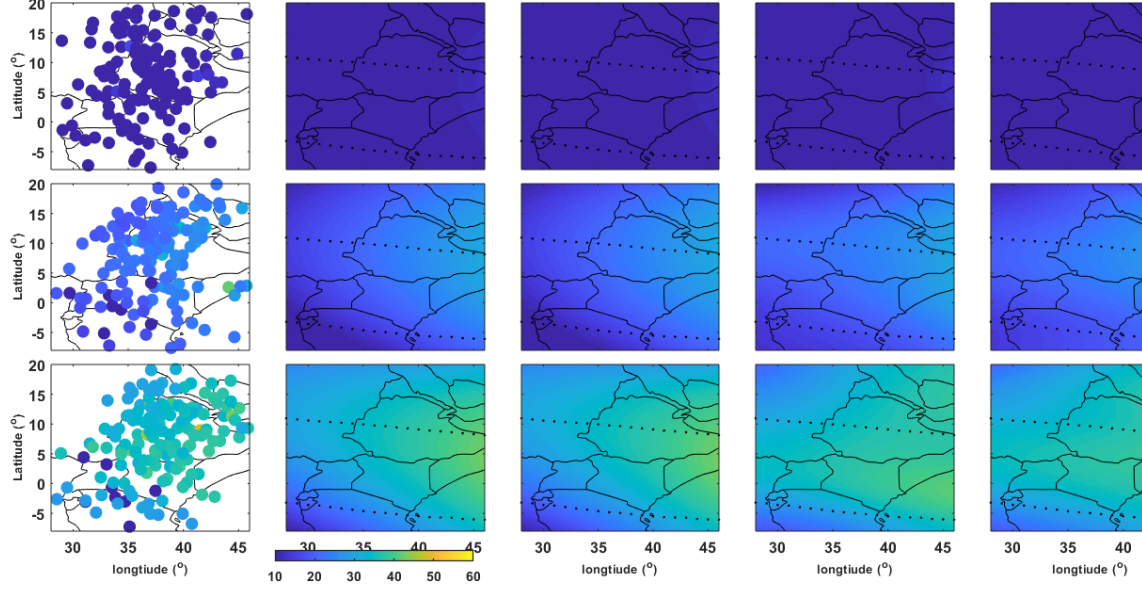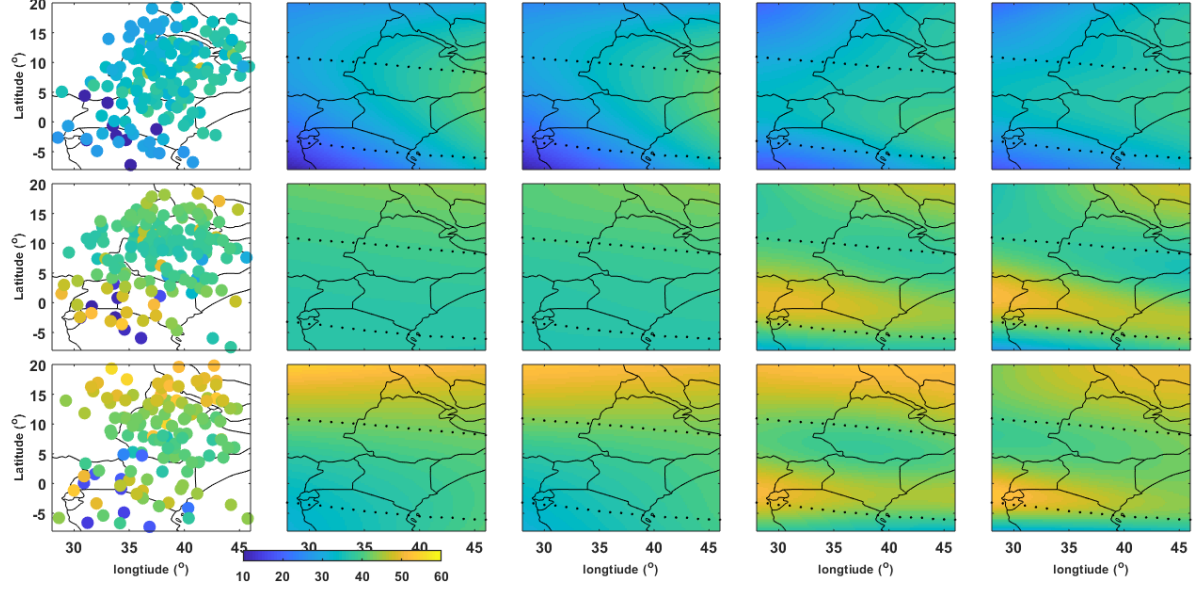
plot.

Figure 4: Scatter plot of experimental VTEC versus latitude and longitude , from top to bottom at 2, 4 & 6 UT (left) , and the corresponding VTEC map from polynomial function (2nd column from left), NTCM derived by Id map (3rd column from left), NN (4th column from left) and NeQuick2 derived by Az (5th column from left) on DOY 110 of 2013.
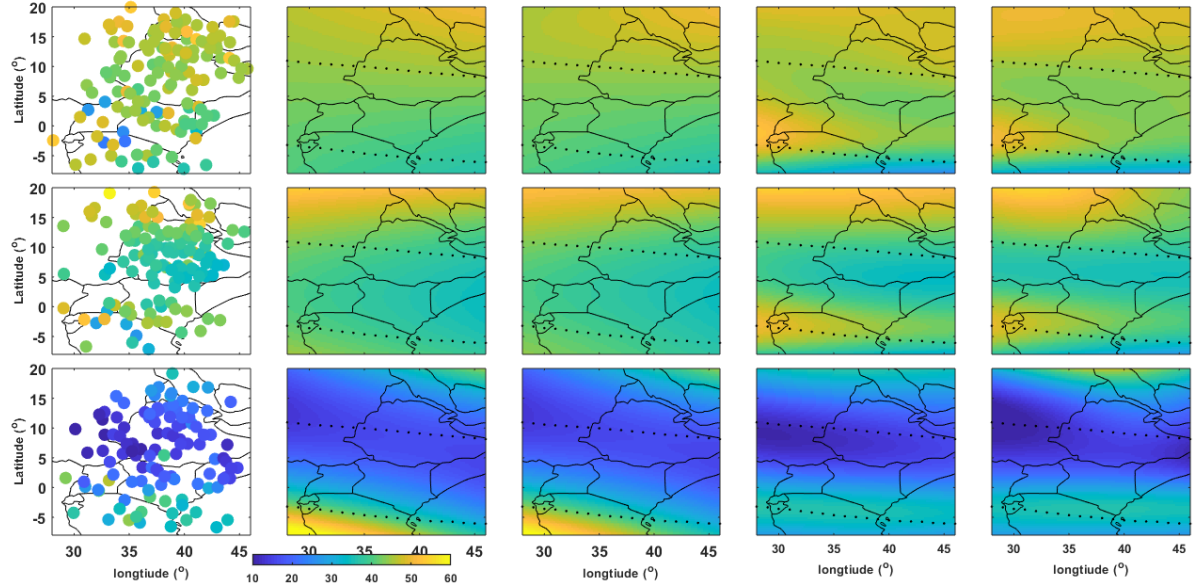
Figure 5: Scatter plot of experimental VTEC versus latitude and longitude , from top to bottom at 8,10 & 12 UT (left) , and the corresponding VTEC map from polynomial function (2nd column from left), NTCM derived by Id map (3rd column from left),NN (4th column from left) and NeQuick2 (5th column from left) on DOY 110 of 2013.

Figure 6: Scatter plot of experimental VTEC versus latitude and longitude , from top to bottom at 14,16 & 18 UT (left) , and the corresponding VTEC map from polynomial function (2$^{\text{nd}}$ column from left), NTCM derived by Id map (3$^{\text{rd}}$ column from left),NN (4$^{\text{th}}$ column from left) and NeQuick2 derived by Az (5$^{\text{th}}$ column from left) on DOY 110 of 2013

4.3 NTCM, NeQuick2 and NN diurnal performances

Panels (a-d) of Figure 7 show the diurnal variations of observed (*red), NTCM modeled (blue), NeQuick2 modeled (*green), and NN modeled (-.black) VTEC at Asab station for the DOYs 80, 170, 266, and 350 in 2015 respectively. The number of observed VTEC at a particular UT might be more than one since it is at IPPs of lines that join the receiver with different possibly observing satellites at the UT. As we can see from the graphs, the models generally reconstruct the pattern of diurnal variation of observed VTEC throughout hours of the day. However, there is a difference in their capability to reproduce VTEC, particularly at around 10 UTC. NTCM and NN models retrieve the VTEC for almost all hours. However, the NeQuick2 model can capture diurnal variations of VTEC for intervals of UTC before and after 8-14 UTCs except for DOY 170.

The second, third, and fourth column panels of Figure 7 display the frequency distributions of mis-modeling of NTCM & NeQuick2 after data ingestion and NN in their order, including the means ( ) and standard deviations ( ) at the Asab station. The mean error range for the NTCM model is 0.02-0.12 TECU. However, for NN and NeQuick2, the mean error ranges are 0 TECU and -0.01 -0.34 TECU, respectively. The standard deviations of errors for the NTCM model range from 2.09 to 5.33 TECU. For the NeQuick2 model it is 3.48 - 4.67 TECU, but for NN, it is 1.20 -2.12 TECU. In general, the means of mis-modeling of NeQuick2 are considerably higher than the means of mis-modeling NTCM and NN. The negative sign of means indicates that the models averagely overestimated the experimental. The standard deviations of mis-modeling for NN are less than their values for NeQuick2 and NTCM (see Figure 7). The NTCM and NN estimate the observation VTEC better than NeQuick2.
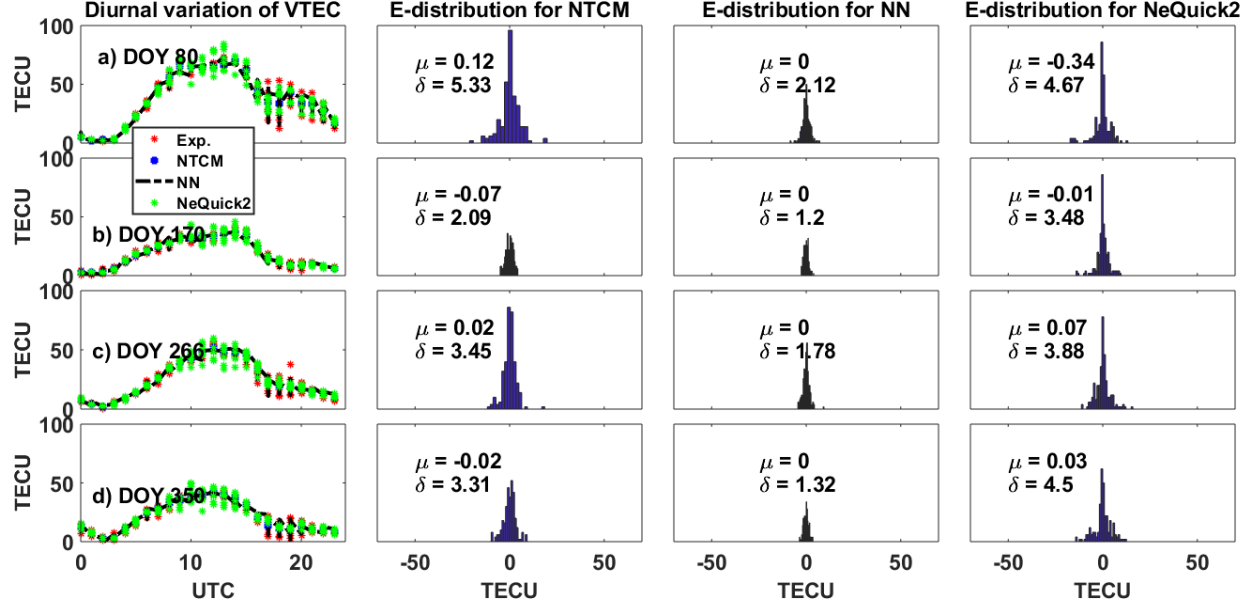
15

Figure 7: Diurnal variation of experimental and modeled (NTCM,NN and NeQuick2) VTEC (left); frequency distribution of mis-modeling of hourly VTEC (second column NTCM, third column NN and fourth column NeQuick2) at Asab station for DOY 80,170,266 and 350 in 2015.

Similarly, we used GPS data from different stations (see Figure 8 and Table 3). Panels (a-b) in Figure 8 indicate that the modeled VTECs agree with the experimental TEC. The frequency distributions of mis-modeling of NTCM, NN and NeQuick2 are almost symmetric near 0 TECU showing a Gaussian distribution. The means and standard deviations, presented in Figure 8 (second column NTCM, third Column NN, and fourth column NeQuick2) and Table 3, quantify the extent of mis-modeling. The means and standard deviations of mis-modeling for NN are significantly less relative to NTCM and NeQuick2. In these stations, NTCM showed better performance than NeQuick2 as NeQuick2 averagely overestimated the experimental VTEC.
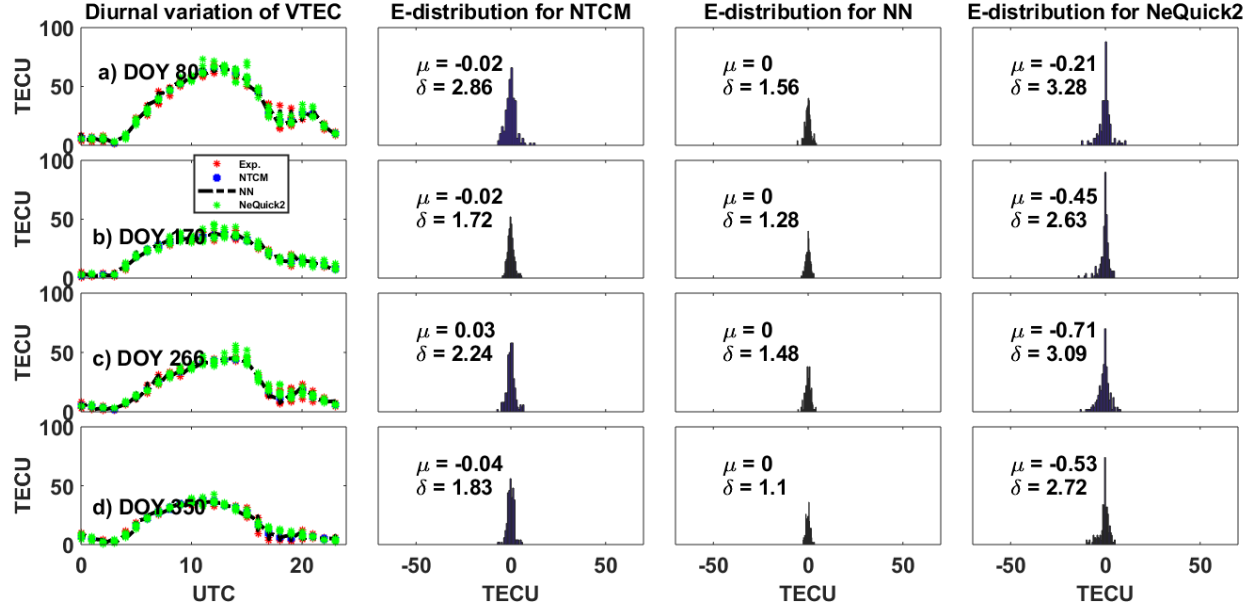
Figure 8 : Diurnal variation of experimental and modeled (NTCM,NN and NeQuick2) VTEC (left); frequency distribution of mis-modeling of hourly VTEC (second column NTCM, third column NN and fourth column NeQuick2) at Arbaminch station for DOY 80,170,266 and 350 in 2015.

Table3: Means and standard deviations of mis-modling of NTCM, NeQuick2 and NN -VTEC for sample stations

stations	Models	NTCM		NeQuick2		NN	
ADIS	DOY	Mean	STD	Mean	STD	Mean	STD
	80	-0.01	4.17	-0.18	4.75	0.00	2.79
	170	0.02	2.50	0.35	3.15	0.00	1.76
	266	-0.02	2.48	-0.02	3.76	-0.01	1.74
	350	0.05	3.21	-0.76	4.28	0.01	2.48
DEBK	80	0.03	4.30	-0.13	4.12	0.00	2.36
	170	-0.01	2.04	-0.06	3.15	0.01	1.19
	266	0.01	3.83	-0.32	4.36	0.01	2.11
	350	0.02	3.20	0.39	4.13	0.01	1.35
MOIU	80	-0.01	6.08	-0.01	4.58	0.00	2.21
	170	-0.06	3.63	0.05	3.40	-0.01	1.61
	266	0.01	4.72	-0.16	3.94	0.01	1.99
	350	0.04	3.08	-0.83	2.75	0.00	1.55
ASOS	80	-0.04	3.47	-0.14	4.14	0.00	1.68
	170	0.00	1.59	0.01	2.33	0.00	1.24
	266	0.00	2.60	-1.34	4.31	0.01	1.32

17

stations	Models	NTCM	NeQuick2	NN			
	350	0.05	2.11	-0.38	3.35	0.00	0.94

4.4 Comparison of NTCM, NeQuick2, and NN performances in predicating VTEC

The primary aim of models is to predict the variation of a parameter ahead of time; therefore, we analyzed the NTCM, NeQuick2, and NN model's prediction capabilities at 1hr, 2hrs, 3hrs, and 4hrs ahead, of DOY 90 in 2015 at Addis Ababa station. We used the Id (for NTCM) and the Az (for NeQuick2) at 1hr, 2hrs, 3hrs, and 4hrs ahead to determine the models VTEC. Similarly, after training the NN model for daily VTEC, its 1hr, 2hrs, 3hrs, and 4hrs prediction capability has been assessed. Figure 9 shows the predicted VTEC with the observed VTEC. Table 4 presents standard deviations of the TEC prediction errors of these models. For 1hr ahead prediction, the performance of NTCM is better than that of NN and NeQuick2 (see Table 4). However, as the time of prediction increases (2hrs, 3hrs, and 4 hrs ahead), their prediction ability reduces. But, the errors for NTCM became higher than for NeQuick2 and NN at two hours (and above) predication. Generally, the model's performances suffer during mid-day time (from 4-15 UTC) as the errors are higher for this time interval.

Time intervals(in hrs)	Error STD in TECU for Models		
	NTCM	NeQuick2	NN
1	8.96	11.11	10.79
2	15.63	14.13	15.23
3	21.80	16.56	19.28
4	27.91	18.83	22.92

Table 4: hourly prediction error STD for NTCM, NN and NN models
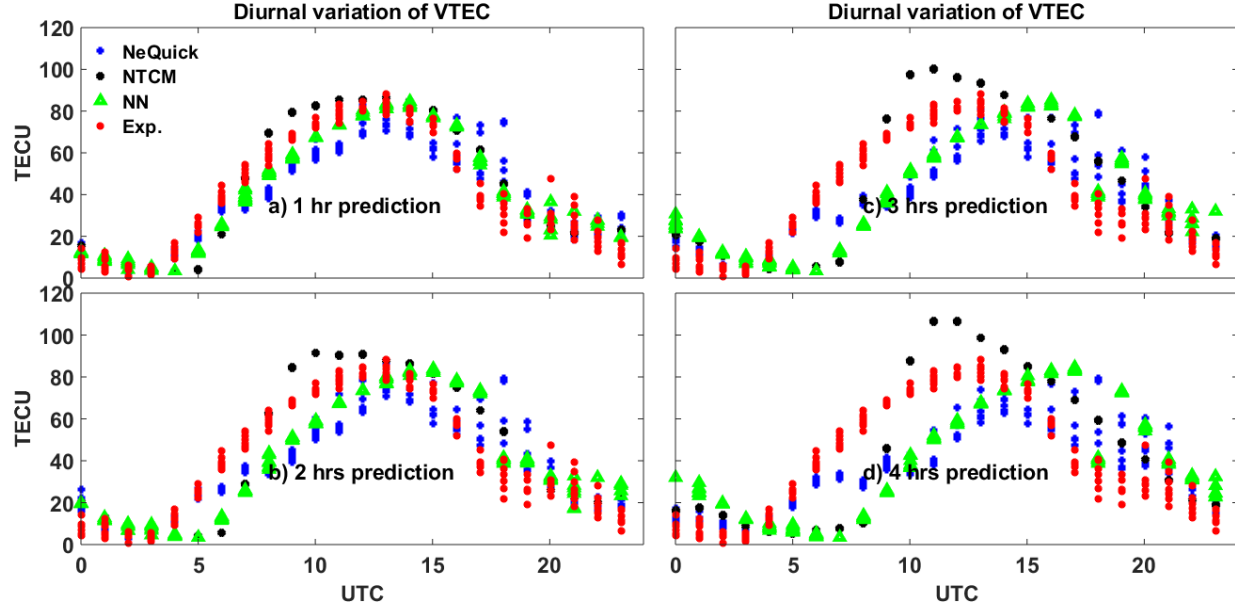
18

Figure 9: Diurnal variation of experimental and predicted model VTEC at Addis Ababa station for DOY 90 in 2015. Panels a,b,c and d are 1hr,2hrs,3hrs and 4hrs time of prediction respectively.

Figure 10 shows the daily variation of standard deviation (STD) of mismodelings of VTEC for ten consecutive days. For both now casting and one day ahead prediction, the performances of NN and NTCM are relatively better than the performance of NeQuick2. Generally, Table 4 and Figure 10 show their performances suffer more for hourly prediction than daily prediction. It agrees with the expectation that hour-to-hour variation of the state of the ionosphere is higher than that of day to day for no random irregularities.
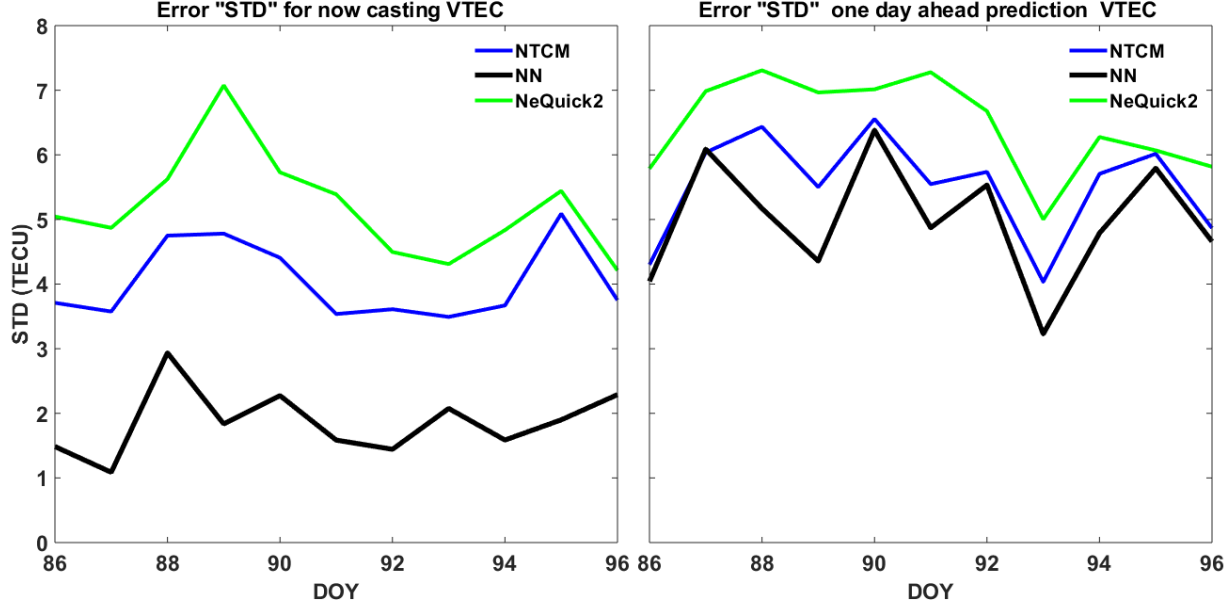
Figure 10: Daily variation of error std a) for now casting VTEC & b) for one day head prediction VTEC at Addis Ababa station in 2015.

To summarize, the performance of NN highly depends on the time length of the data used. In the case of extended time data, as NN tries to capture the dominant variation by ignoring small changes in the data, its performance is reduced. However, in the case of short-time data, it reproduces more details of changes in VTEC, and therefore, its performance becomes high. As data ingestion works point by point for the data used, the performance of NTCM and NeQuick2 models cannot be much affected by the data used. Since we used extended data for the annual case, NN's performance is relatively weaker than NTCM's and comparable to NeQuick2's. However, for VTEC mapping, NN could perform better than NTCM and comparably to NeQuick2. For diurnal nowcasting, NN is best to capture the experimental TEC, which may be due to the limited data variation. For the case of one day ahead prediction, NN showed better performance than that of the other models. However, for the prediction of an hour ahead, its performance is comparable to the other models.

5 Conclusions

As the ionosphere empirical models such as NeQuick2, NTCM, and NN have various mathematical expressions, their complexity and performances in describing the ionosphere of different sectors are not the same. However, there is a demand for a simple, fast and effective model to specify the state of the ionosphere. We have evaluated the GPS- VTEC-assisted NTCM model performance compared to the adapted NeQuick2 and NN models in characterizing the East African ionosphere. We have assessed their annual, diurnal, mapping, and prediction

20

performances. The result showed that the NTCM model performs better than the NeQuick2 model and NN for annual VTEC reconstructions. The correlation coefficient (R) values for the NTCM model and observed VTEC are higher than for NN and NeQuick2. The STDs and RMSEs for NTCM are smaller than for NN and NeQuick2. In the case of diurnal, NN is the best model for capturing experimental VTEC. However, for mapping VTEC the performance of NN is better than NTCM and comparable to that of the NeQuick2 model. The models could capture the observed EIA in the region. However, NN and NeQuick2 models capture the EIA more clearly than NTCM and the Interpolation technique. For hourly prediction, their performances are weaker than their daily prediction performances. Overall, the performance of NN varies with the extent of the data used. Therefore, it seems that, since NTCM is simple & fast to use and its performance when it is assisted by GPS data is comparable to (in some cases better than) other models, it might be a good candidate model to study the East-African ionosphere.

References

B. D.L. Opperman , P. J. Cilliers , L. McKinnell , R. Haggard (2007), Development of a regional GPS- based ionospheric TEC model for South Africa., Advances in Space Research.

Bilitza, D. (2018), IRI the international standard for the ionosphere, Adv. Radio Sci.,

https://doi.org/10.5194/ars-16-1-2018.

Brunini, C., Azpilicueta,F., Gende ,M. Camilion, E., Aragón-Ángel, A. Hernandez-Pajares ,M. ,

Juan ,M., Sanz ,J., Dagoberto Salazar (2011), Ground- and space-based GPS data

ingestion into the NeQuick model, *J.Geod.,* doi: 10.1007/s00190-011-0452-4.

Burden, F., Winkler, D., 2009. Bayesian Regularization of neural networks. In: Livingstone, D.J. (Ed.), Artificial Neural Networks: Methods and Applications. Humana Press, pp. 23–42.

http://dx.doi.org/10.1007/978-1-60327-101-1_3.

Ciraolo, L., F. Azpilicueta, C. Brunini, A. Meza, and S. M. Radicella (2007), Calibration

errors on experimental slant total electron content (TEC) determined with GPS, *J. Geod., 81, 111–120.*

D.J. (Ed.), Artificial Neural Networks: Methods and Applications. Humana Press, pp. 23–42.

http://dx.doi.org/10.1007/978-1-60327-101-1__3.

Davies, K. (1990), Ionosphere Radio, *Peter Peregrinus Ltd., London*, doi:10.1049/PBEW031E.

Di Giovanni, G., and S. M. Radicella (1990), An analytical model of the electron density profile

in the ionosphere, *Adv. Space Res., 10, 27 –30.*

Duhoux, M., Suykens, J., De Moor, B., Vandewalle, J.(2001), Improved long-term temperature

prediction by chaining of neural networks. Int. J. Neural syst. 11 (01),1–10.

Ercha Aa, Aaron Ridley, Wengeng Huang, Shasha Zou, Siqing Liu, Anthea J. Coster, and

Shunrong Zhang (2018), An Ionosphere Specification Technique Based on Data Ingestion

Algorithm and Empirical Orthogonal Function Analysis Method, American *Geophysical*

Union, doi: 10.1029/2018SW001987.

Fausett, L.(1994), Fundamentals of Neural Networks; Architectures Algorithms and Applications.

Prentice-Hall, Inc., New Jersey, 076324,

Foresee, F.D., Hagan, M.T., (1997). Gauss-Newton approximation to Bayesian learning. In: Neural

Networks, 1997., International Conference on, vol. 3, pp. 1930–1935.

Getahun, B. and Nigussie, M. (2021), Performance of GPS-TEC assisted NTCM-model to describe the East-African Equatorial ionosphere, Adv. Space Res. 68, Issue 11,p.4665-4677.

DOI:10.1016/j.asr.2021.08.029.

Ghosh, S., Doshi-Velez, F. (2017), Model selection in Bayesian neural networks via horseshoe priors. ArXiv e-prints.

Habarulema, J.B., McKinnell, L.A., Cilliers, P.J. (2007), Prediction of Global Positioning System total electron content using neural networks over South Africa. J. Atmos. Sol. Terr. Phys. 69 (15),

1842–1850.

Habarulema, J.B., McKinnell, L.-A., Cilliers, P.J., Ben Opperman, D.L.(2009), Application of

neural networks to South African GPS TEC modelling. Adv. Space Res. 43, 1711–1720.

http://dx.doi.org/10.1016/j.asr.2008.08.020.

Haykin, S. (1999), Neural Networks: A comprehensive foundation, 2nd Edition Prentice Hall, Upper

Saddle River, USA.

Hernández-Lobato, J.M., Adams, R. (2015), Probabilistic backpropagation for scalable learning of

Bayesian neural networks. In: Bach, F., Blei, D. (Eds.), Proceedings of the 32nd International Conference on Machine Learning, vol. 37. Proceedings of Machine Learning Research, pp. 1861–1869. In: Neural Networks, 1997., International Conference on, vol. 3, pp. 1930–1935.

Jakowski, N., C. Mayer, C. Borries, and V. Wilken, Space weather monitoring by ground and space based GNSS measurements, Proc. ION – International Technical Meeting, January 26–28, Anaheim, CA, 2009.

Jakowski, N., M. M. Hoque and C. Mayer (2011), A new global TEC model for estimating

transionospheric radio wave propagation errors , J.Geod., doi :10.1007/s00190-011-0455-1.

Jakowski, N., Y.Beniguel, G. De Franschi, M.H. Pajares, K.S. Jaconsen, I.Stanislawska, L. Tomasik, R.Waranant, G. Wautelet (2012), Monitoring, tracking and forecasting ionosphere

perturbation using GNSS techniques, J. Space Weather Space Climate,

DOI: 10.1051/SWSC/2012022

Khan, M.S., Coulibaly, P. (2006), Bayesian neural network for rainfall-runoff modeling.Water Resour. Res. 42 (7).

Kouris,S.S., TH.D. Xenos,K.V. Polimeris and D. Stergiou(2004): TEC and foF2 variations:

pre-liminary results, Ann. Geophysics,47(4), (in press)

Lamming, X., Cander, L.R. (1999), Monthly median fof2 modeling cost 251 area by neural networks.

Phys. Chem. Earth Part C: Solar Terr. Planet. Sci. 24 (4), 349–354.

http://dx.doi.org/10.1016/S1464-1917(99)00010-0.

MacKay, D.J.C. (1992), A practical bayesian framework for backpropagation networks.

Neural Comput. 4 (3), 448–472. http://dx.doi.org/10.1162/neco.1992.4.3.448.

Mannucci, A. J., B. D. Wilson, D. N. Yuan, C. H. Ho, U. J. Lindqwister, and T. F. Runge (1998),

A global mapping technique for GPS-derived ionospheric total electron content

measurements, *Radio Sci., 33, 565–582*, doi:10.1029/97RS02707.

Nava, B., P. Coïsson, and S. M. Radicella (2008), A new version of the NeQuick ionosphere

electron density model, J. Atmos. Sol. Terr. Phys., 70, 1856–1862,

doi:10.1016/j.jastp.2008.01.015.

Nava, B., Radicella, S. M., & Azpilicueta, F. (2011), Data ingestion into NeQuick 2, *Radio*

Science, *46, RS0D17*, doi: 1029/2010RS004635.

Nava, B., S. M. Radicella, R. Leitinger, and P. Coïsson (2006), A near real-time model-assisted

ionosphere electron density retrieval method, *Radio Sci., 41, RS6S16*, doi:

10.1029/2005RS003386.

Nigussie, M., S. M. Radicella, B. Damtie, B. Nava, E. Yizengaw, and L. Ciraolo (2012), TEC

ingestion into NeQuick 2 to model the East African equatorial ionosphere, *Radio Sci., 47,*

RS5002, doi:10.1029/2012RS004981.

Poole, A.W., McKinnell, L.-A (2000), On the predictability of foF2 using neural networks. Radio Sci. 35 (1), 225–234.

Razin, M.R.G., Voosoghi, B., Mohammadzadeh, A.(2016), Efficiency of artificial neural networks in map of total electron content over iran. Acta Geod. Geophys. 51,541–555.

http://dx.doi.org/10.1007/s40328-015-0143-3.

Scherliess, L., R. W. Schunk, J. J. Sojka, and D. Thompson (2004), Development of a physics-based reduced state Kalman filter for the ionosphere, Radio Sci., 39 (RS1S04),

doi:10.1029/2002RS002797.

Sojka, J. J., D. C. Thompson, L. Scherliess, and R. W. Schunk (2007), Assessing models for ionospheric weather specification over Australia

during the 2004 CAWSES campaign, J. Geophys. Res., 112, A09306, doi:10.1029/2006JA012048.

Soudry, D., Meir, R. (2013), Mean field bayes backpropagation: scalable training of multilayer neural networks with binary weights. ArXiv e-prints arXiv:1310.1867.

Tebabal, A., Radicella, S.M., Damtie, B., Y. Migoya-Orue, Nigussie, M., Nava, B. (2019), Feed

forward neural network based ionospheric model for the East African region. J. Atmos.

Sol. Terr.Phys.

Tebabal, A., Radicella, S.M., Nigussie, M., Damtie, B., Nava, B., Yizengaw, E. (2018), Local

TEC modeling and forecasting using neural networks. J. Atmos. Sol. Terr.Phys. 172, 143–

151.

Tiwari, R., Strangeways, H.J., Tiwari, S., Ahemad, A. (2013), Investigation of ionospheric

irregularities and scintillation using TEC in highlatitude, *Adv. Space Res. 52, 1111–1124.*

Tulunay, E., E. T. Senalp, L. R. Cander, Y. K. Tulunay, A. H. Bilge, E. Mizrahi, S. S. Kouris, and N. Jakowski (2004), Development of algorithms and software for forecasting, nowcasting and variability of TEC, Ann. Geophys., 47(2 − 3), 1201 − 1214.

Tulunay, E., E. T. Senalp, S. M. Radicella, Y. Tulunay (2006), Forecasting total electron content maps by neural network technique, Radio science, DIO: 10.1029/2005RS003285.